Electrochemical Modeling of Electron and Proton Transfer to Ubiquinone-10 in a Self-Assembled Phospholipid Monolayer

Maria Rosa Moncelli, Lucia Becucci, Andrew Nelson, and Rolando Guidelli
Chemistry Department, University of Florence, Florence 50121, Italy

ABSTRACT Ubiquinone-10 (UQ) was incorporated at concentrations ranging from 0.5 to 2 mol% in a self-assembled monolayer of dioleoylphosphatidylcholine (DOPC) deposited on a mercury drop electrode, and its electroreduction to ubiquinol (UQH_2) was investigated in phosphate and borate buffers over the pH range from 7 to 9.5 by a computerized chronocoulometric technique. The dependence of the applied potential for a constant value of the faradaic charge due to UQ reduction upon the electrolysis time t at constant pH and upon pH at constant t was examined on the basis of a general kinetic approach. This permitted us to conclude that the reduction of UQ to UQH_2 in DOPC monolayers takes place via the reversible uptake of one electron with the formation of the semiubiquinone radical anion $UQ^{\cdot -}$, followed by the rate-determining protonation of this anion with $UQH^{\cdot}$ formation; this neutral radical is more easily reduced than UQ, yielding the ubiquinol UQH_2. In spite of the very low concentration of hydrogen ions as compared with that of the acidic component of the buffer, the only effective proton donor is the proton itself; this strongly suggests that the protonation step takes place inside the polar head region of the DOPC monolayer, which is only accessible to protons.

INTRODUCTION

Ubiquinone-10 (UQ) is a hydrophobic molecule with a long, somewhat rigid, isoprenoid side chain of 50 Å associated with the mitochondrial membrane at a concentration that normally falls in the range of 1–2 mol%. Ever since the development of the chemiosmotic theory and the citation of UQ as the primary transporter of protons across the mitochondrial membrane resulting from electron transfer, there has been intense interest in the mechanism of its function (Mitchell, 1976). In spite of this activity many questions about the properties of UQ, in particular its electrochemistry, remain to be resolved. The reason for this is that up to now there has not been a reliable membrane model available for the observation of the electron- and proton-transferring properties of UQ. The main efforts have been limited to aqueous-organic (Morrison et al., 1982) and nonaqueous solutions (Prince et al., 1983). More recent studies have focused on looking at the electrochemical properties of UQ adsorbed on pyrolytic graphite (Shrebler et al., 1990), mercury (Gordillo and Schiffrin, 1994), and *n*-alkanethiol modified gold electrodes (Takehara et al., 1991). At the same time, the electrochemical behavior of UQ within a phospholipid layer deposited on an alkane-thiol modified gold electrode (Laval and Majda, 1994) and within a thick phospholipidic matrix applied to a pyrolytic graphite electrode (Sánchez et al., 1995) has been studied. The use of a membrane model to investigate UQ behavior is very important, because the location of UQ within phospholipid membranes (Stidham et al., 1984) and its lateral mobility are critical to its function (Laval and Majda, 1994). Indeed, the characteristics of the mobility of UQ within lipid bilayers and biological membranes and the relation of this mobility to the electron- and proton-transferring properties of the UQ molecule is still associated with much controversy (Rajarathnam et al., 1989). In addition to these properties of UQ, the hydrophobicity and hydrogen-binding capability of quinones have been proposed as being important to their electron and proton transfer abilities in lipidic membrane environments. These characteristics affect the manner whereby UQ partitions within the membrane phase. They also influence the way in which the polar functional quinone group contacts the aqueous phase and binds to redox-active proteins for proton and electron transfer, respectively (Rich and Harper, 1990).

A novel membrane model has recently been developed whereby stable, reproducible phospholipid and modified phospholipid monolayers can be deposited on mercury electrodes and their electrochemical properties examined with high precision and accuracy (Nelson and Benton, 1986; Moncelli et al., 1994; Moncelli and Becucci, 1995). The lipid coating is provided by spreading a solution of the lipid in a suitable solvent (e.g., pentane) on the surface of an aqueous electrolyte, allowing the solvent to evaporate, and immersing a hanging mercury drop electrode in the electrolyte. The validity of a lipid film supported by a metal as a biomimetic membrane can be assessed by comparing its properties with those of planar bilayer lipid membranes (BLMs). The differential capacity of phospholipid films deposited on mercury drops ranges from 1.6 to 1.8 $\mu F\ cm^{-2}$, depending on the nature of the lipid and on the experimental conditions, and hence is about twice as high as that of BLMs, thus confirming their nature of self-assembled half-membranes, with the polar heads directed toward the bathing solution (Nelson and Benton, 1986). As distinct

Received for publication 5 June 1995 and in final form 7 March 1996.

Address reprint requests to Dr. Rolando Guidelli, Laboratorio di Elettrochimica, University of Florence, Via G. Capponi 9, Florence 50121, Italy. Tel.: 39-55-2757540; Fax: 39-55-244102; E-mail: guidelli@cesit1.unifi.it.

Dr. Nelson is on leave from Plymouth Marine Laboratory, Citadel Hill, Plymouth, PL1 2PB, England.

0006-3495/96/06/2716/11 $2.00

from usual planar BLMs, these lipid monolayers are completely solvent-free, and hence are characterized by very low values ($\leq 5 \times 10^{-2}$ V^{-2}) of the fractional increase in differential capacity per square volt, α (Alvarez and Latorre, 1978); this prevents detectable changes in their thickness, and hence in their differential capacity, with a change in the potential difference across the film. Moreover, these mercury-supported monolayers provide an inherent mechanical stability and a resistance to high electric fields that is not shared by BLMs.

By an accurate design of the stationary mercury electrode and of the cell, the differential capacity C of these films can be measured with an accuracy better than 0.02 μF cm^{-2}. This permitted us to appreciate the changes in C caused by a change in the ionic surface potential ψ after a change in the electrolyte concentration (Moncelli et al., 1994). The intrinsic pK_a values of the ionizable groups of phosphatidylcoline (PC) and phosphatidylethanolamine (PE) films as estimated from these differential capacity measurements agree with those obtained by using different membrane models, including vesicles and planar BLMs. The only remarkable discrepancy concerns the charge density of phosphatidylserine (PS) monolayers deposited on mercury, which passes from slight negative to slight positive values as the pH is decreased from 7.5 to 3. The latter behavior, which is not shared by PS vesicles, can be explained by the existence of at least two different conformations of the polar heads of PS self-organized films, with similar Gibbs energies but quite different acidities of the ionizable groups (Moncelli et al., 1994, and references therein). This interpretation seems to be confirmed by the observation that these PS films behave as though they were negatively charged when in the presence of lipophilic cations incorporated in the film (Moncelli et al., 1995). Tetraphenylphosphonium cations (tetraphenylborate anions) incorporated into these PC and PS monolayers tend to accumulate in the polar head region at the more positive (negative) applied potentials; a sufficiently large potential step in the negative (positive) direction may cause these lipophilic ions to translocate from the polar head region to the electrode surface. By measuring the charge after such a step at different concentrations of the lipophilic ions, it was possible to determine their adsorption isotherms in the polar head region of the lipid. The adsorption coefficient of tetraphenylborate in PC monolayers, 6.3×10^{-3} cm, was thus found to be in fairly good agreement with that determined on BLMs (see Moncelli et al., 1995, and references therein). The reproducibility of these lipid monolayers and the sensitivity of the electrochemical techniques employed allowed the determination of adsorption coefficients as low as 2.5×10^{-5} cm, such as that of tetraphenylphosphonium ion in PC monolayers.

A variant of this lipid-coated mercury electrode, suggested by the pioneering work by Miller (1981), permits us to establish the location of lipophilic ions within the film. If the neck of the mercury drop is kept in contact with the lipid film previously spread on the solution surface, the lipid monolayer that coats the drop surface remains in equilibrium with this "lipid reservoir" and hence retains its properties upon contraction of the drop surface. Consequently, the charge flowing along the external circuit as a consequence of this contraction provides a measure of the charge density σ_M on the mercury surface, with an accuracy of 0.02 μC cm^{-2}. If the applied potential is kept constant, σ_M remains substantially unaffected by the presence of lipophilic ions in the polar head region, because by far the major contribution to the potential difference across the lipid film is located in the hydrocarbon tail region. On the contrary, if the lipophilic ions are directly adsorbed on the electrode surface, the σ_M value differs from that measured at the same applied potential in the absence of these ions by an amount that is practically equal to the opposite of the charge borne by the ions. This method permitted us to distinguish unequivocally the uninteresting situation in which lipophilic ions are in direct contact with the mercury surface from the much more relevant situation in which they are located in the polar head region (Moncelli et al., J. Electroanal. Chem. In press). All of the above results show unequivocally that lipid monolayers on mercury, besides being very reproducible and stable, are well characterized as representing exactly half a bilayer.

One major advantage of lipid monolayers deposited on mercury over lipid films deposited on solid electrodes is represented by the liquid state of mercury, which provides a perfectly smooth and defect-free support to the lipid film. All solid electrodes, even if carefully polished, exhibit a high density of surface defects such as steps, kinks, adatoms, and vacancies. Moreover, by far the majority of these electrodes are polycrystalline, and hence exhibit grain boundaries. The best lipid films deposited on solid electrodes are obtained by anchoring the -SH group of long-chain aliphatic tiols to the surface of a carefully polished gold electrode to form a tiol monolayer, and by then forming a bilayer by Langmuir-Blodgett transfer of a second monolayer of phospholipid (Laval and Majda, 1994). However, even these bilayers exhibit pinhole defects, probably induced by the surface defects of the metal substrate; these pinhole defects, with a mean separation estimated at about 50 Å, may provide direct access of lipophilic species such as UQ to the electrode surface. More frequently, lipid films with incorporated UQ or other lipophilic species are obtained by spreading a solution of the lipid and of the lipophilic species in a suitable solvent on the surface of the solid electrode and by allowing the solvent to evaporate (Ksenzhek et al., 1982; Sánchez et al., 1995); the amount of lipid material is notably in excess with respect to that required to form a monolayer, and hence multilayers with a poorly defined structure are formed. The mode of transport of reducible lipophilic species across these films may therefore be quite different from that across self-assembled mono- or bilayers.

An advantageous feature of self-assembled lipid monolayers deposited on mercury is represented by the fact that the metal behaves like a lipophobic redox couple O/R, the

redox standard potential $E^{\circ}_{O/R}$ of which can be varied at will and in a continuous way by varying the applied potential. Thus, the electrochemical potential $\tilde{\mu}_{e,O/R}$ of electrons in a redox couple varies linearly with its redox standard potential for a constant ratio of the concentrations of the oxidized and reduced species (Walz, 1979); likewise, the electrochemical potential $\hat{\mu}_{e,M}$ of electrons in a metal M varies linearly with its applied potential E. Thus, switching the applied potential from a value negative enough to electroreduce the oxidized form O′ of a lipophilic redox couple O′/R′ incorporated in the lipid film to a value positive enough to electrooxidize the reduced form R′ amounts to replacing a lipophobic redox couple O/R with $E^{\circ}_{O/R} < E^{\circ}_{O'/R'}$ by one with $E^{\circ}_{O/R} > E^{\circ}_{O'/R'}$ on one side of the film. Any protons involved in the reduction of the lipophilic redox couple O′/R′ are provided on the other side of the lipid film, i.e., on the solution side. A quantitative analysis of the mechanism by which an important mitochondrial redox component of the electron-transport chain such as UQ is electroreduced while being incorporated into a self-organized and practically defect-free lipid monolayer in contact with an aqueous solution is therefore of significance from a biophysical viewpoint, because it simulates biologically relevant conditions. This is even more significant because, as distinct from many model systems reported in the literature in which mole fractions of UQ less than 10% have rarely been used (Katsikas and Quinn, 1981, 1982a,b; Alonso et al., 1981), UQ concentrations as low as 0.5 mol% have been adopted. The electrochemical behavior of UQ has been investigated as a function of its concentration in the lipid layer, the solution pH, and the concentration of solution buffer. Particular attention has been paid to understanding the mechanism of the reduction in terms of the rate-determining steps and the relation of this mechanism to the location of UQ in the lipid layer.

MATERIALS AND METHODS

The adsorbed monolayers of dioleoyl lecithin (DOPC) on mercury were prepared as described earlier (Nelson and Benton, 1986; Moncelli et al., 1994; Moncelli and Becucci, 1995). The water used was obtained from light mineral water by distilling it once, and by then distilling the water so obtained from alkaline permanganate, while constantly discarding the heads. Merck reagent grade KCl was baked at 500°C before use to remove any organic impurities. DOPC was obtained from Lipid Products (South Nutfield, Surrey, England). Ubiquinone-10 (UQ) was derived from horse heart (Sigma) and was used without further purification. UQ was dissolved in pentane and stored at −20°C. Working solutions of lipid and UQ were prepared in pentane for spreading at the air-water interface every 3 days and stored at −20°C. All measurements were carried out in aqueous 0.1 M KCl at 25°C. The pH was controlled with the NaH_2PO_4/Na_2HPO_4 buffer from 7 to 8 and with the $HBO_2/NaBO_2$ buffer from 7.5 to 9.5. The overall concentration of the acidic and basic components of the buffer is referred to as the buffer concentration.

The home-made hanging mercury drop electrode employed in the measurements, the cell, and the detailed procedure to produce self-organized lipid monolayers deposited on mercury are described elsewhere (Moncelli et al., 1994; Moncelli and Becucci, 1995). Differential capacity measurements were carried out with a Metrohm Polarecord E506 (Herisau, Switzerland). The AC signal had a 10-mV amplitude and a 75-Hz frequency. The system was calibrated with a precision capacitor. All potentials were measured versus a saturated calomel electrode (SCE). A chronocoulometric procedure described elsewhere (Moncelli et al., 1995) was employed to study electron transfer to the UQ molecule using a wholly computerized apparatus (Foresti et al., 1980). The microprocessor used to control all of the operations was a model NOVA 4X from Data General (Westboro, MA), and an Amel model 551 (Milano, Italy) fast rise potentiostat with a rise time 0.1 μs was employed for the potentiostatic control of the three-electrode system. The detailed scheme of the home-made electronic current integrator working under microprocessor control is described by Carlà et al. (1988).

Each chronocoulomogram consisted of a series of consecutive potential jumps of progressively increasing height from a fixed initial value E_i, which was set equal to −100 mV/SCE unless otherwise stated, to different final values of E_f, ranging from −100 to −600 mV, and was recorded on a single lipid-coated mercury drop. The charge $Q(t)$ after each potential jump $E_i \rightarrow E_f$ was recorded versus the time t elapsed from the instant of the jump for 50 ms, after which the potential was stepped back to E_i, where it remained for 1 s. During this period the reduction product of UQ was completely reconverted to UQ. Thus, an increase in the rest time at E_i beyond 1 s left the charge $Q(t)$ practically unaltered. It should be noted that the initial potential cannot be made more positive than −100 mV, because at more positive potentials the lipid monolayer becomes permeable to inorganic ions and can no longer be regarded as a biomimetic membrane. This limits the accessible pH range to pH values ≥ 7, because at lower pH values the reoxidation of the product of UQ reduction to UQ would require an initial potential more positive than −100 mV. The reoxidation to UQ at $E_i = -100$ mV is relatively slow in the time scale of 50 ms; this is the reason why chronocoulomograms obtained by choosing an initial potential negative enough to cause the complete reduction of UQ (say, $E_i = -700$ mV) and by stepping toward progressively more positive potentials show no indication of a reoxidation to UQ.

The curves of the differential capacity C of the phospholipid monolayers deposited on mercury were constantly measured against the applied potential E after the recording of each chronocoulomogram. Each series of chronocoulometric measurements at different buffer concentrations and constant pH or at different pH values and constant concentration of the acidic component of the buffer was carried out on a single lipid-coated mercury drop or else by using a newly formed drop for each chronocoulomogram. In the first case a slight but detectable increase in capacity was observed in passing from the first to the last chronocoulomogram of the series. Hence, the following results refer to series carried out by recording each chronocoulomogram on a different lipid-coated mercury drop.

The charge density σ_M on the lipid-coated mercury drop at constant applied potential was estimated by contracting the drop surface by an accurately measured amount while keeping its neck in contact with the (lipid + UQ) layer at the argon/solution interphase, and by recording the charge flowing along the external circuit as a consequence of this contraction.

RESULTS

Fig. 1 shows a series of curves of the charge $Q(t)$ after the potential jump −100 mV → E_f as a function of the time t elapsed from the instant of the jump, for several final potentials E_f, as provided by a DOPC monolayer containing 0.5 mol% UQ. At the less negative E_f values at which UQ is still electroinactive, the charge $Q(t)$ increases abruptly in less than 1 ms, because of the flow of the capacitive current that is required to charge the interphase, and then attains a time-independent value. At more negative E_f values $Q(t)$ increases in time first abruptly, because of the capacitive contribution, and then more slowly, because of the gradual electroreduction of UQ in time. With a further gradual shift of E_f toward negative values, the electroreduction rate of

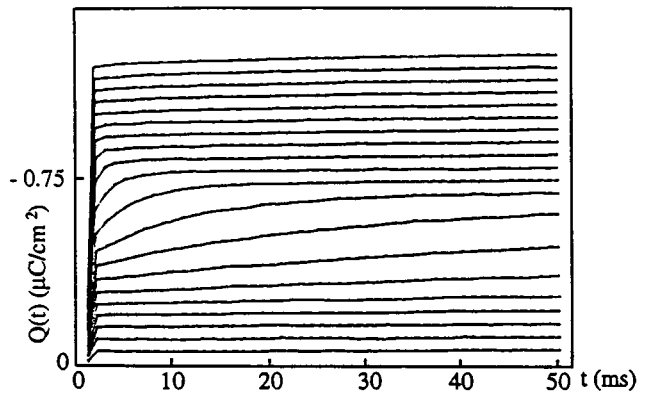

FIGURE 1 $Q(E_f,t)$ versus t curves for 1 mol% UQ reduction in a 0.075 M borate buffer of pH 9.4, as obtained by stepping the potential from a fixed initial value $E_i = -0.200$ V to final values E_f varying from −0.225 to −0.700V by 25-mV increments.

UQ increases progressively, until ultimately the UQ incorporated in the lipid monolayer is completely reduced in less than 1 ms, after which $Q(t)$ attains once again a time-independent value.

Fig. 2 shows a series of curves of $Q(t = 50$ ms) versus E_f at pH 8 for different UQ concentrations ranging from 0.5 to 2 mol%. These curves are sigmoidal in shape, with a rising portion preceded by a sloping foot and followed by a sloping plateau. The foot and the plateau are practically parallel, and their common slope is a measure of the differential capacity of the lipid monolayer. The faradaic contribution $Q_f(t)$ to $Q(t)$ due to the reduction of UQ is readily estimated by measuring the charge from the straight line obtained by extrapolation of the foot of the $Q(t)$ versus E_f curve, as indicated in Fig. 2, curve *a*. The maximum limiting value $Q_{f,max}$ attained by $Q_f(t)$ along the plateau is clearly independent of the electrolysis time t and measures the maximum charge involved in the reduction of the UQ incorporated into the film. The inset of Fig. 2 shows a plot of $Q_{f,max}$ versus the UQ concentration. At the lowest UQ concentration (0.5 mol%), $Q_{f,max}$ is practically equal to the charge estimated for the complete two-electron reduction of UQ to the ubiquinol UQH_2, assuming that both the lipid and the UQ molecules occupy a surface area of 65 Å^2. Incidentally, at the low UQ concentrations investigated, the uncertainty in the actual surface area a occupied by one UQ molecule has an almost negligible effect on such an estimate. Thus, for a UQ concentration of 1 mol% in the lipid monolayer, there is one UQ molecule over an area of $(99 \times 65 + a)$ Å^2 of the film; the number of UQ molecules per unit surface is therefore equal to $1/(99 \times 65 + a)$ Å^{-2}, which is practically equal to $1/(99 \times 65)$Å^{-2}, independent of the particular orientation of the UQ molecule with respect to the plane of the lipid film.

As the UQ concentration is increased from 0.5 to 2 mol%, the $Q_{f,max}$ value starts to deviate from the estimated value, as appears from the inset of Fig. 2. The C versus E curve obtained with 0.5 mol% UQ incorporated in the DOPC film practically coincides with that obtained for pure DOPC; in particular, the differential capacity along the flat minimum in the C versus E curve assumes the same value of about 1.75 μF cm^{-2} for both cases. With an increase in the UQ concentration a single immersion of the mercury drop through the layer of (DOPC + UQ) spread on the argon/solution interface turned out to be insufficient to attain the same differential capacity minimum as that of a pure DOPC monolayer. To achieve this goal, an increasing number of successive immersions of the same mercury drop was normally required. The chronocoulomograms in Fig. 2 were recorded after attaining this result. At UQ concentrations higher than 2 mol%, experimental measurements became

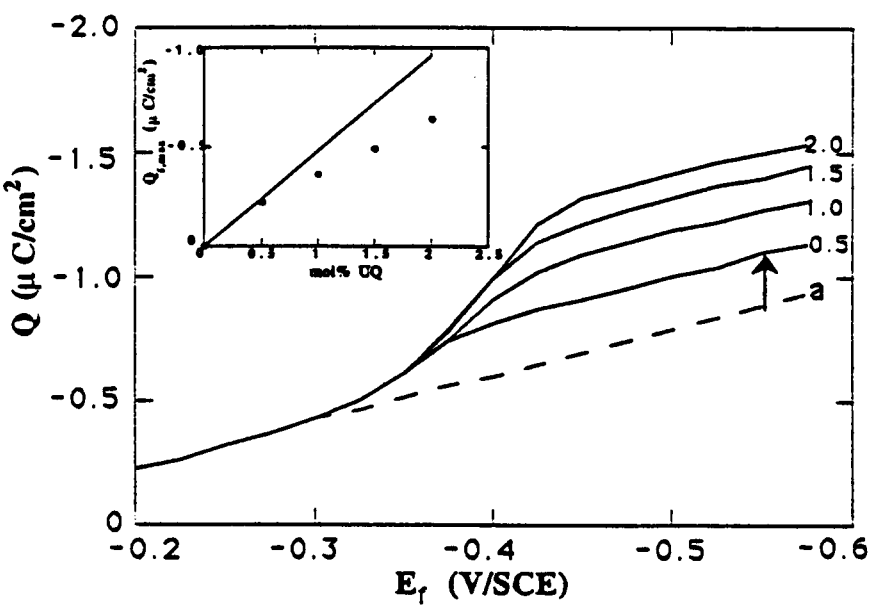

FIGURE 2 $Q(t = 50$ ms) versus E_f plots for UQ reduction in a 0.01 M borate buffer of pH 8. The number on each curve denotes the mol% UQ in the DOPC monolayer. The dashed curve *a* was obtained by extrapolating the foot of the $Q(t = 50$ ms) versus E_f curves. The inset shows a plot of $Q_{f,max}$ versus the UQ concentration; the straight line was calculated as described in the text.

progressively more irreproducible, even when the above procedure was adopted. In what follows all results refer to 0.5 mol% UQ in the lipid monolayer.

Fig. 3 shows a series of $Q(t)$ versus E_f curves at different electrolysis times t and at constant pH and buffer concentration, whereas Fig. 4 shows curves at different pH values while keeping both t and the concentration of the acidic component of the borate buffer constant. It is apparent that an increase in pH causes a negative shift in the reduction potential of UQ. Over the whole pH range investigated, a change in the buffer concentration from 5×10^{-4} to 5×10^{-2} M at constant pH has no appreciable effect on UQ reduction.

The charge density σ_M on the DOPC-coated mercury drop was measured both in the absence and in the presence of UQ at potentials along the foot, the rising portion, and the plateau of the Q_f versus E_f curves. At all potentials investigated the presence of 0.5 mol% UQ was found to have no effect on the σ_M value within the accuracy of our measurements ($\sim$0.02 μC cm^{-2}). The major contribution to the potential difference across the interface is made by the potential difference across the hydrocarbon tail region of the lipid, which is approximately given by $4\pi(\sigma_M + \sigma_i)d/\epsilon_t$, where d and $\epsilon_t \approx 2$ are the thickness and the dielectric constant of this region and σ_i is the charge density of any charged species directly adsorbed on the mercury surface. The fact that σ_M at constant applied potential does not change upon incorporation of UQ implies that σ_i is very small, and hence that the headgroups of the products of partial and total reduction of UQ are either uncharged or else localize somewhere in the polar head region of the lipid monolayer.

DISCUSSION

A variety of techniques have been applied to understand the physical organization and orientation of UQ in a membrane, but a general consensus among researchers has yet to emerge. The most widely accepted model suggests that the isoprene tail and the quinone ring lie in the midplane of the bilayer (Quinn and Esfahani, 1980; Katsikas and Quinn, 1982a; Ondarroa and Quinn, 1986; Ulrich et al., 1984; Cornell et al., 1987), whereas another model places the isoprene tail in the midplane but the headgroup in the polar head region, where it can have access to the membrane surface (Mitchell, 1976; Stidham et al., 1984). The view is widely accepted that a large fraction of UQ segregates within the membrane into a phase that is not constrained by the ordered chains of the membrane lipid, but there is disagreement regarding the UQ mole fraction beyond which such a segregation occurs. Thus Cornell et al. (1987) conclude that UQ segregates at concentrations as low as 0.02 mol% and that the physiologically active UQ reaching the reaction site may be only a small fraction of the total separate UQ. Conversely, according to Stidham et al. (1984), only limited amounts of added UQ enter the bilayer, and much of the UQ is in a separate, "UQ-rich" phase; the modest effects of added UQ on the physical properties of the bilayer should be attributed to the membrane-associated fraction of UQ. The maximum incorporation of UQ in liposomes is estimated at about 5 mol% by Stidham et al. (1984) and at 2 mol% by Kingsley and Feigenson (1981); this quantity should be substantially intercalated in the bilayer lipids. The fact that all UQ molecules incorporated in our DOPC monolayer at a 0.5 mol% concentration are electroreduced to ubiquinol in less than 1 ms after a suffi-

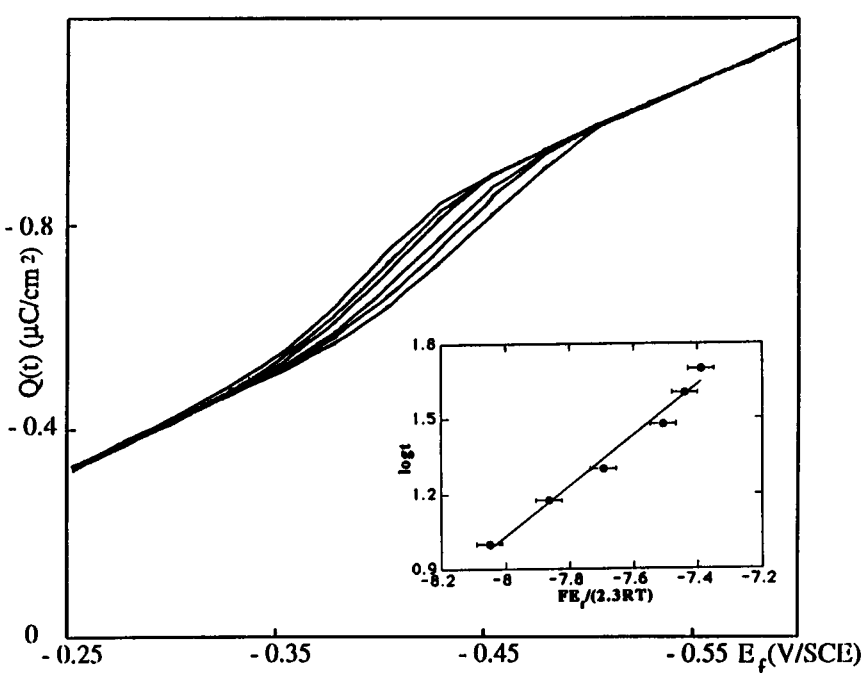

FIGURE 3 $Q(t)$ versus E_f curves for 0.5 mol% UQ reduction at different electrolysis times t in a 10^{-3} M borate buffer of pH 7.9. From right to left t takes the values 10, 15, 20, 30, 40, and 50 ms. The inset shows a plot of log t versus $FE_f/(2.3RT)$ as obtained at $Q_f = -0.10$ μC/cm^2 from the chronocoulomogram in the figure. The solid curve in the inset has unit slope.

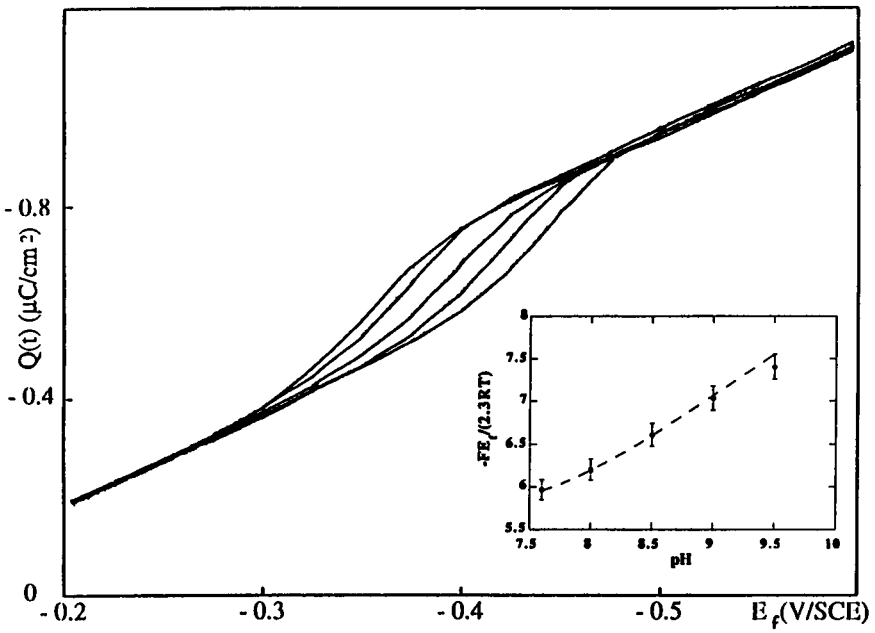

FIGURE 4 $Q(t = 50\ \text{ms})$ versus E_f curves for 0.5 mol% UQ reduction in borate buffers of constant concentration, 10^{-2} M, of HBO_2 and different pH values. From left to right the pH varies from 7.5 to 9.5 by 0.5 increments. The inset shows a plot of $-FE_f/(2.3RT)$ versus pH as obtained at $Q_f = -0.10\ \mu C/cm^2$ from the chronocoulomograms in the figure. The dashed curve in the inset was obtained from Eq. 16 with $K_{ads} = 4 \times 10^7$ liter mol^{-1} and was shifted vertically to attain the best overlap with the experimental plot.

ciently negative potential step lends support to the view that at these low concentrations the UQ molecules are actually intercalated in the lipid molecules and therefore are in a condition favorable to their electroreduction. The modest deviations from a complete two-electron reduction of UQ as observed over the range of UQ concentrations from 0.5 to 2 mol% (see the inset of Fig. 2) may possibly be ascribed to an incipient segregation of UQ molecules. The difficulties met in obtaining reproducible results for still higher UQ concentrations in the (lipid + UQ) layer deposited at the argon/solution interface are probably due to the appearance of a new UQ-rich phase in this layer. The necessity of passing the mercury drop a few times across this (lipid + UQ) layer, even over the range of UQ concentrations from 0.5 to 2 mol%, to transfer to the mercury drop a lipid monolayer with the same features as those of a pure monolayer, may also be ascribed to the tendency of the UQ molecules to segregate; repeated immersions may favor the intercalation of these molecules in the lipid monolayer.

For a quantitative interpretation of the experimental behavior let us first adopt a general approach that holds strictly for a sequence of elementary electron transfer and heterogeneous chemical steps involving the various intermediates as well as any proton donors, under the assumption that all of these steps take place at the same distance from the electrode surface and that all changes in the applied potential E are entirely localized across this distance. The moderate deviations from the predictions of this model will then be discussed and justified.

An electrode reaction, just like a redox reaction, will generally consist of a series of consecutive elementary steps; some of these steps are necessarily electron transfer steps, whereas some others may be chemical in nature. In the reduction of organic compounds, by far the most common chemical steps are "protonation" steps, i.e., steps involving the uptake of one proton. Under steady-state conditions all consecutive steps proceed at the same rate v, but one of them (the rate-determining step, rds) is normally characterized by a much higher rate constant than the others. When this is the case, the forward and backward rates of all other elementary steps are much greater than their difference, which equals the common net rate v. The forward rate of each of these steps may therefore be equated to the corresponding backward rate to a good degree of approximation, leading to equilibrium conditions for all steps other than the rds. Let the algebraic sum of all elementary steps preceding the rate-determining one be expressed by the general equation

$$r\,\mathrm{R} + h\,\mathrm{H}^+ + \tilde{n}e^- \Leftrightarrow \mathrm{I}. \qquad (1)$$

Here R denotes the reactant UQ, r and h are stoichiometric coefficients, $\tilde{n}$ is the number of electrons exchanged before the rds, and I is the intermediate involved in the rds. Upon applying the equilibrium conditions to the sum of the steps in Eq. 1 we get

$$a_\mathrm{I} = K a_\mathrm{R}^r a_{\mathrm{H}^+}^h \exp\left(-\frac{\tilde{n}FE_f}{RT}\right), \qquad (2)$$

where a_R, a_I, $a_{\mathrm{H}+}$ are the activities of R, I, H^+, and K is an equilibrium constant. If is $\tilde{n} \neq 0$, Eq. 2 is an application of the Nernst equation to the "quasi equilibrium" of Eq. 1, because in the present case UQ exchanges electrons with the electrode, rather than with another redox couple. Conversely, if $\tilde{n}$ equals zero, Eq. 2 is just an application of the law of mass action.

Let us ascribe to the rds involving the intermediate I the general form

$$i\mathrm{I} + h'\mathrm{H}^+ + \delta e^- \rightarrow \text{products}. \qquad (3)$$

Here i and h' are the molecularities of the rds with respect to the intermediate I and to the protons, respectively. The general Eq. 3 includes as particular cases: 1) an electron transfer step if $i = \delta = 1$ and $h' = 0$; 2) a protonation step if $i = h' = 1$ and $\delta = 0$; 3) a dimerization or a disproportionation step if $i = 2$ and $h' = \delta = 0$. The rate v of the rds, which is also the rate of the overall process, is given by

$$v = \frac{j}{nF} = -\frac{d\Gamma_R}{dt} = \frac{k}{f_{\neq}} a_I^i \exp\left(-\delta \frac{\beta F E_f}{RT}\right). \quad (4)$$

Here j is the current density, n is the number of electrons involved in the overall reduction of one reactant molecule (2 in the present case), Γ_R is the concentration of R, k is a rate constant, and $f_{\neq}$ is the activity coefficient of the activated complex for the rds.

If the rds is an electron transfer step (i.e., if $\delta = i = 1$ and $h' = 0$), then the exponential factor in Eq. 4 expresses the exponential dependence of the rate of this step upon the applied potential E_f. Here β is the "symmetry factor": it is a measure of the probability of the transferring electron being in the molecule of the intermediate I in the transition state, whereas $(1 - \beta)$ is the probability of its being in the metal (Hush, 1958). The symmetry factor is the equivalent for electrode reactions of the Brønsted coefficient for homologous homogeneous reactions (Krishtalik, 1986) and takes values that are close to 0.5.

If the rds is a protonation step (i.e., if $\delta = 0$ and $i = h' = 1$) and different proton donors A_iH have access to the reaction site, then the rate constant k in Eq. 4 has the general form

$$k = \sum_{A_iH} k_{A_iH} a_{A_iH}^{h'}, \quad (5)$$

where the summation is extended to all proton donors in view of general acid-base catalysis. In practice, the buffered solution ensures the constancy of the activities a_{AiH} of all proton donors just outside the lipid monolayer during electrolysis.

On substituting a_I from Eq. 2 into Eq. 4, setting $a_R = f_R\Gamma_R$ and integrating by separation of variables we get

$$\int_{\Gamma_R(t)}^{\Gamma_R(0)} \frac{f_{\neq}}{f_R^{ri}} \frac{d\Gamma_R}{\Gamma_R^{ri}} = kK^i a_{H^+}^{ih} \exp\left[-(i\vec{n} + \delta\beta)\frac{FE_f}{RT}\right]t. \quad (6)$$

Here $\Gamma_R(0)$ and $\Gamma_R(t)$ are the concentrations of UQ before the electrolysis and at time t, respectively, and f_R is its activity coefficient.

A convenient way to make use of Eq. 6 consists of adjusting the experimental conditions in such a way as to keep the integral on the left-hand side constant. This goal is achieved by carrying out the kinetic analysis at a constant initial concentration of UQ (and hence at constant $\Gamma_R(0)$) and at a constant value of the faradaic charge $Q_f(t)$, which follows the potential jump $E_i \rightarrow E_f$ and consumes the reactant R. In fact, by definition, $Q_f(t)$ is given by

$$Q_f(t) = \int_0^t j(t)\,dt = -nF\int_0^t \frac{d\Gamma_R}{dt}\,dt = nF[\Gamma_R(0) - \Gamma_R(t)], \quad (7)$$

and hence a constant value of $Q_f(t)$ implies a constant value of $\Gamma_R(t)$. As concerns the two activity coefficients $f_{\neq}$ and f_R under the integral sign in Eq. 6, in principle they are functions of the concentrations of all reacting species in the lipid monolayer. In practice, however, the concentrations of all intermediates, because of their transitory nature, can be disregarded with respect to the concentration $\Gamma_R(t)$ of the reactant R, and that, $\Gamma_P \approx \Gamma_R(0) - \Gamma_R(t)$, of the final product P. Therefore, the experimental strategy consists of measuring the dependence of E_f upon the electrolysis time t at constant pH and upon pH at constant t, while the initial UQ concentration and $Q_f(t)$, and hence the concentrations of the various reacting species within the lipid layer, are kept constant. In particular, if t and E_f are both varied so as to keep $Q_f(t)$ constant, then the resulting constancy of both members of Eq. 6 permits us to write

$$\frac{RT}{F}\left(\frac{\partial \ln t}{\partial E_f}\right)_{pH=const} = i\vec{n} + \delta\beta, \quad (8)$$

at constant $\Gamma_R(0)$, $Q_f(t)$, and pH. On the other hand, if the rds is not a protonation step, so that k is independent of pH, and we adjust E_f and the solution pH so as to keep Q_f constant, then Eq. 6 yields

$$\frac{F}{RT}\left(\frac{\partial E_f}{\partial pH}\right)_{t=const} = -2.303\frac{ih}{(i\vec{n} + \delta\beta)}, \quad (9)$$

at constant $\Gamma_R(0)$, $Q_f(t)$, and t. In view of Eqs. 5 and 6, the presence of a rate-determining protonation step is revealed by a change in E_f when the buffer concentration is varied while keeping pH, $\Gamma_R(0)$, Q_f, and t constant, unless the proton itself is the only effective proton donor. In the latter case the rate of change of E_f with varying pH will be given by

$$\frac{F}{RT}\left(\frac{\partial E_f}{\partial pH}\right)_{t=const} = -2.303\frac{(ih + h')}{(i\vec{n} + \delta\beta)}. \quad (10)$$

The inset of Fig. 3 shows a plot of log t versus $FE_f/(2.3RT)$ over the t range from 10 to 50 ms, as obtained at $Q_f = -0.1\ \mu C\ cm^{-2}$ from the chronocoulomogram in the same figure. This plot is roughly linear and exhibits a slope that is practically equal to unity. Unit slopes were obtained at all pH values investigated. The plot of $-FE_f/(2.3RT)$ versus pH as obtained at $Q_f = -0.1\ \mu C\ cm^{-2}$ and $t = 50$ ms from a series of chronocoulomograms in different $HBO_2/NaBO_2$ buffered solutions of constant HBO_2 concentration is also approximately linear, with a slope of about 0.8 (see the inset of Fig. 4).

In view of Eq. 8, the unit slope of the experimental log t versus $FE_f/(2.3RT)$ plots indicates that the quantity $i\vec{n} + \delta\beta$ is also equal to unity. This implies that $\vec{n} = i = 1$ and $\delta = 0$, and hence that the rds is a chemical step after the reversible uptake of the first transferring electron. In fact, if the rds were the first or the second electron transfer step, then $i\vec{n} + \delta\beta$ would be approximately equal to 0.5 or to 1.5, respectively. We must also exclude a rate-determining chemical step consisting of a dimerization or a disproportionation of the intermediate I, because otherwise we would have $i = 2$. The fact that the slope of the $-FE_f/(2.3RT)$ versus pH plot is close to unity can be justified either on the basis of Eq. 9 with $h = i = 1$, or on the basis of Eq. 10 with $h = 0$ and $h' = 1$. However, in the former case the rds would be preceded by both an electron transfer and a protonation step (see Eq. 1), and we would be left with a rate-determining chemical step that can be neither a dimerization nor a disproportionation step. Nor can the rds be a protonation step, because the $-FE_f/(2.3RT)$ versus pH plot would then have a slope equal to 2. In view of the difficulty of envisaging another plausible rate-determining chemical step, the most logical conclusion consists of regarding $h = 0$ and $h' = 1$ in Eq. 10. This amounts to concluding that the chemical rds is a protonation step involving the proton as the only effective proton donor. Summarizing, the mechanism emerging from the above considerations is as follows:

$$\mathrm{UQ} + e \leftrightarrow \mathrm{UQ}^{\cdot-};\ \mathrm{UQ}^{\cdot-} + \mathrm{H}^+ \overset{\text{rds}}{\rightarrow} \mathrm{UQH}^{\cdot};$$
$$\mathrm{UQH}^{\cdot} + \mathrm{H}^+ + e \leftrightarrow \mathrm{UQH_2}. \qquad (11)$$

The slight deviations of the $-FE_f/(2.3RT)$ versus pH plot from the predictions of Eq. 10 can be rationalized on the basis of the following considerations. In the electroreduction of organic compounds that are strongly adsorbed on mercury in the absence of a lipid film, the acidic component HA_i of the buffer makes an appreciable direct contribution to the rate of any rate-determining protonation steps (Guidelli, 1971); at the relatively high pH values adopted herein, this contribution is often greater than that of the hydroxonium ions and satisfies Eq. 5. The fact that the reduction of UQ incorporated into a DOPC monolayer does not depend on the buffer concentration at constant pH, and hence does not satisfy the principles of general acid-base catalysis, can only be explained by assuming that the protonation takes place well inside the polar head region of the DOPC monolayer, which is practically impermeable to the HBO_2 molecules within the time scale of the experiment, while it may be permeated by the proton itself, possibly but not necessarily aquated. In this case the role of the buffer is exclusively that of maintaining the pH just outside the lipid layer constant during UQ reduction, through a dissociation reaction in quasi-equilibrium. Hence, the rate-determining protonation step is affected by a change in pH, but not by a change in the buffer concentration at constant pH.

It should be pointed out that the general approach leading to Eqs. 8–10 relies on the assumption that the elementary steps preceding the rds are in quasi-equilibrium at the location where the rds takes place. If we assume that the rate-determining protonation step takes place well inside the polar head region, and hence close to the boundary between this region and the adjacent hydrocarbon tail region, then we must also assume that any translocation of the electroactive moiety of the UQ molecule, namely its quinone ring, across the hydrocarbon tail region is fast in the time scale of our chronocoulometric measurements, so as to be regarded as in quasi-equilibrium. According to Stidham et al. (1984), the quinone ring of the UQ molecule (henceforth briefly referred to as UQ unless otherwise stated) in lipid bilayers is located at the boundary between the hydrocarbon tail region and the polar head region. Although an electron tunneling across the hydrocarbon tail region cannot be excluded a priori, it appears improbable. Thus, the height of the energy barrier across which the electron must tunnel decreases progressively as the difference between the applied potential E_f and the redox standard potential of the reducing species (i.e., the overpotential η) becomes more negative (Lipkowski et al., 1986). At a lipid-coated mercury electrode some evidence of electron tunneling is only observed with species (such as Fe^{3+}) whose overpotential is < -0.5 V (Moncelli et al., unpublished results). Conversely, the electroreduction of UQ submonolayers deposited directly on a mercury electrode (Gordillo and Schiffrin, 1994) takes place at potentials that are only about 0.2 V more positive than those at which the UQ incorporated into our lipid monolayer is electroreduced. If we exclude electron tunneling across the hydrocarbon tail region, UQ must translocate across this region to the mercury surface to undergo the first electronation, and the resulting anion radical $UQ^{\cdot-}$ must then translocate back to the boundary between the hydrocarbon tail region and the polar head region to undergo protonation. The assumption that such a translocation is in quasi-equilibrium in the time scale of 50 ms is consistent with the observation that the translocation of several lipophilic ions across lipid monolayers and bilayers takes place in less than 1 ms (Läuger et al., 1981). Note that if both the electron transfer from the mercury to UQ and the subsequent translocation of the resulting $UQ^{\cdot-}$ anion across the hydrocarbon tail region to the protonation site are in quasi-equilibrium, then the electric potential difference that is effective in the combination of these two consecutive steps is not the potential difference $\Delta\phi$ across the whole interphase, but is that ($\Delta\phi_t$) across the hydrocarbon tail region. The potential difference across the diffuse layer adjacent to the lipid film is almost negligible under the present conditions, because the DOPC monolayer is electrically neutral and the electrolyte concentration is relatively high. Hence we can set $\Delta\phi = E_f + \text{const.} \approx \Delta\phi_t + \Delta\phi_h$, where $\Delta\phi_h$ is the potential difference across the polar head region and account has been taken of the fact that the applied potential E_f differs from $\Delta\phi$ by a constant (const.) that depends exclusively on the choice of the reference

electrode. If in Eq. 6 we set $i = \tilde{n} = 1$, $\delta = h = 0$, $k = k_{H+}a_{H+}$ and we replace E_f by $\Delta\phi_t = E_f + \text{const.} - \Delta\phi_h$, we obtain

$$a_{H^+} \exp\left[-\frac{F}{RT}(E_f - \Delta\phi_h)\right] t = \text{constant} \quad \text{for } \Gamma_R(0) \text{ and } Q_f \text{ constant.} \tag{12}$$

The rate-determining protonation step involves the passage of the protons from the bathing solution to the protonation site across the polar head region. In a formal way we may represent such a passage as an adsorption step. Let us assume that this step is in quasi-equilibrium. In this case the activity a_{H+} of protons in the protonation site, which we will henceforth identify for simplicity with its concentration Γ_{H+} within the polar heads, will be related to the hydrogen ion concentration c_{H+} outside the lipid layer via an adsorption isotherm. If this isotherm is linear (Henry isotherm), it can be written as

$$a_{H^+} \approx \Gamma_{H^+} = K_{ads} \exp\left(-\frac{F}{RT}\Delta\phi_h\right) c_{H^+}, \tag{13}$$

where K_{ads} is the chemical contribution to the adsorption coefficient, whereas $\exp(-F\Delta\phi_h/RT)$ is the electrostatic contribution accounting for the electrical work required to move the proton across the polar head region. On substituting a_{H+} from Eq. 13 into Eq. 12, we obtain

$$c_{H^+} \exp\left(-\frac{F}{RT}E_f\right) t = \text{constant} \quad \text{for } \Gamma_R(0) \text{ and } Q_f \text{ constant.} \tag{14}$$

It is apparent that a linear adsorption isotherm cannot explain the observed deviation of the slope of the $-FE_f/(2.3RT)$ versus pH plot in Fig. 4 from unity. It is interesting to observe that Eq. 14 does not depend on the particular position within the polar head region where protonation takes place; while one fraction of the potential difference $\Delta\phi$ across the whole interface assists the electron transfer to UQ and the translocation of the resulting $UQ^{\cdot -}$ anion to the protonation site, the remaining fraction assists the passage of the proton from the solution to the same protonation site.

A slope of the $-FE_f/(2.3RT)$ versus pH plot of slightly less than unity can be predicted if the experimental increase in c_{H+} from $\sim 10^{-9}$ to $\sim 10^{-7}$ M causes Γ_{H+} to approach a saturation value, $\Gamma_{H+,max}$. The simplest isotherm predicting the attainment of a saturation value is the Langmuir isotherm:

$$\frac{\theta_{H^+}}{1 - \theta_{H^+}} = K_{ads} \exp\left(-\frac{F}{RT}\Delta\phi_h\right) c_{H^+} \quad \text{with } \theta_{H^+} = \frac{\Gamma_{H^+}}{\Gamma_{H^+,max}}. \tag{15}$$

If we substitute $a_{H+} = \theta_{H+}\Gamma_{H+,max}$ from this isotherm into Eq. 12 we obtain

$$\frac{c_{H^+}}{1 + K_{ads} \exp(-F\Delta\phi_h/RT) c_{H^+}} \exp\left(-\frac{F}{RT}E_f\right) t = \text{constant} \quad \text{for } \Gamma_R(0) \text{ and } Q_f \text{ constant.} \tag{16}$$

According to this equation, $\exp(FE_f/RT)$ at constant t increases with c_{H+} less than proportionally, provided that the second term in the denominator is not negligibly small with respect to unity. Thus, for $K_{ads} = 4 \times 10^7$ liter mol^{-1}, Eq. 16 yields a $-FE_f/(2.3RT)$ versus pH plot which over the pH range from 7.5 to 9.5 is only slightly curved, with an average slope of about 0.8 (see the dashed curve in the inset of Fig. 4). As expected, the slope of this calculated plot tends to unity with an increase in pH. In principle, because of the presence of the $\exp(-F\Delta\phi_h/RT)$ factor, Eq. 16 also predicts a deviation of the slope of log t versus $FE_f/(2.3RT)$ plots at constant pH from the unit value. In practice, however, the influence of this factor is entirely negligible. Thus, the potential range covered in a log t versus $FE_f/(2.3RT)$ plot is about 40 mV; because the potential difference across the two polar head regions of a lipid bilayer is normally less than 5% of the potential difference across the whole bilayer (Andersen et al., 1978; Flewelling and Hubbell, 1986), the concomitant change in $\Delta\phi_h$ is expected to be only a few millivolts.

The redox potential for the UQ/UQH_2 couple at pH 7 in our lipid monolayer, −0.32 V/SCE, is practically identical to that (−0.33 V against an Ag/sat. AgCl electrode) determined by cyclic voltammetry from a UQ solution in methanol (Bauscher and Mäntele, 1992), where UQ reduction to UQH_2 takes place in a single wave. Conversely, the reduction of *p*-quinones in aprotic solvents gives rise to two consecutive one-electron waves due to the formation of the semiquinone monoanion and the quinol dianion, respectively. In particular, the first wave for UQ reduction from a tetrahydrofurane solution is shifted by 0.8 V in the negative direction with respect to the single two-electron wave in methanol, once potentials are referred to the solvent-independent redox potential of ferrocene.

In view of its insolubility in water, redox potentials of UQ in aqueous solutions can only be determined in the adsorbed state. Ksenzhek et al. (1982) deposited a UQ film on pyrolytic graphite from a toluene solution containing an amount of UQ corresponding to about 10 monolayers, whereas Shrebler and Sánchez et al. deposited on the same electrode material an amount of UQ about one order of magnitude larger from benzene (Shrebler et al., 1990) or chlorophorm + ether solutions (Sánchez et al., 1995). More controlled conditions were adopted by Gordillo and Schiffrin (1994), who deposited submonolayers of UQ on a mercury drop by immersing it through a layer of UQ adsorbed at the air-water interface. Contrasting results have been obtained by these different procedures. Thus, Ksenzhek et al. (1982) found that over the pH range from 0 to 10 UQ reduction proceeds in two steps; moreover, semiubiquinone and

ubiquinol are exclusively present in the totally protonated forms $UQH^{\cdot}$ and UQH_2. This result is somewhat surprising because, as a rule, the *p*-semiquinones $QH^{\cdot}$ in the protonated form are reduced at more positive potentials than the corresponding *p*-quinones Q (Bauscher and Mäntele, 1992): the second electron should therefore be transferred at the same applied potential at which the first electron transfer takes place, yielding directly QH^- or QH_2. On the other hand, according to Schrebler et al. (1990), UQ is directly converted to the ubiquinol anion UQH^- over the pH range from 4.5 to 7.5, whereas from pH 7.5 to pH 11.5 it is reduced in two consecutive one-electron steps to $UQ^{\cdot -}$ and UQH^-, respectively. Finally, Gordillo and Schiffrin (1994) conclude that UQ is directly reduced to the wholly protonated ubiquinol UQH_2 from pH 4 to pH 12. The above differences in behavior are probably to be ascribed to the different conditions under which the adsorbed UQ films were prepared; these conditions may give rise to different structures, which in turn may exhibit a different behavior toward electroreduction. Discrepancies are particularly relevent between the results by Ksenzhek et al. (1982) and those by Sánchez et al. (1995), because they were obtained on the same electrode material, albeit by depositing quite different amounts of UQ per unit electrode surface from different solvents. Both Ksenzhek et al. (1982) and Sánchez et al. (1995) also investigated the reduction behavior of UQ in PC matrixes on pyrolitic graphite under the same experimental conditions adopted by these authors with UQ alone. The conclusions drawn by Ksenzhek et al. (1982) and by Sánchez et al. (1995) about the redox properties of UQ incorporated in PC matrixes are quite different, because they are qualitatively analogous to those reported by the same authors for UQ alone. Moreover, at pH < 6 the presence of PC increases the stability region of semiubiquinone, in the *E* versus pH diagram according to Sánchez et al. (1995), whereas it decreases it according to Ksenzhek et al. (1982). It is possible that the large amount of UQ per unit electrode surface employed by both authors may have favored the segregation of a separate UQ phase, causing UQ reduction to take place primarily across this phase, and the numerous defects in the ill-defined structure of the lipid matrix may have also been a factor. This may explain the modest changes in the redox properties of UQ upon addition of PC as reported by both authors.

Independent of whether adsorbed UQ in direct contact with an aqueous solution may give rise to an anionic or a neutral semiubiquinone or ubiquinol upon electroreduction, our results with UQ incorporated in a lipid monolayer indicate that over the whole pH range investigated the semiubiquinone anion $UQ^{\cdot -}$ is unstable and undergoes a protonation yielding $UQH^{\cdot}$; because this intermediate product is more easily reduced than UQ, in agreement with the general behavior of *p*-quinones, a direct two-electron reduction to ubiquinol takes place. Although our measurements of the charge density σ_M on mercury point out that the final product cannot be the UQH^- anion with the benzenoid ring in direct contact with the electrode surface, in principle we cannot exclude the possibility of the formation of this anionic product if its headgroup locates in the polar head region. In practice, however, this event is highly improbable, in view of the particular conditions realized in a lipid layer. Thus, on the one hand the low dielectric permittivity of the lipidic environment destabilizes charged species in favor of neutral ones, and hence shifts the redox potentials of the $UQ/UQ^{\cdot -}$ and $UQH^{\cdot}/UQH^-$ couples in the negative direction, just as in the case of aprotic solvents. On the other hand, as distinct from the situation in bulk aprotic solvents, the free access of protons from the aqueous phase to the polar head region of the lipid film allows a protonation of the negatively charged species therein; protonated neutral species are therefore expected to be more stable in a lipid film than in an aqueous environment.

Transposition of results obtained in a purely lipidic environment to a "native" environment where the thermodynamic properties of UQ can be modified by different noncovalent binding interactions to proteins must be made with some caution. However, any scheme of proton and electron transport in the respiratory chain envisaging a two-step electroreduction of UQ at two different sites requires quite probably that the diffusion of the semiubiquinone radical anion $UQ^{\cdot -}$ between the two sites be faster than its protonation. In fact, a protonation much faster than diffusion would cause the uptake of two electrons at a single site.

Further work will concentrate on looking at the effect of different lipids and lipid mixtures and at the role of UQ as a mediator of electron transport across lipid monolayers.

During the period of this work, AN was funded by a British Council-MURST grant. The financial support of the Ministero dell'Università e della Ricerca Scientifica e Tecnologica and of the Consiglio Nazionale delle Ricerche is gratefully acknowledged.

REFERENCES

Alonso, A., J. C. Gomez-Fernandez, F. J. Aranda, F. J. F. Belda, and F. M. Goni. 1981. On the interaction of ubiquinones with phospholipid bilayers. *FEBS Lett.* 132:19–22.

Alvarez, O., and R. Latorre. 1978. Voltage-dependent capacitance in lipid bilayers made from monolayers. *Biophys. J.* 21:1–17.

Andersen, O. S., S. Feldberg, H. Nakadomari, S. Levy, and S. McLaughlin. 1978. Electrostatic interactions among hydrophobic ions in lipid bilayer membranes. *Biophys. J.* 21:35–80.

Bauscher, M., and W. Mäntele. 1992. Electrochemical and infrared-spectroscopic characterization of redox reactions of p-quinones. *J. Phys. Chem.* 96:11101–11108.

Bauscher, M., E. Nabedryk, K. Bagley, J. Breton, and W. Mäntele. 1990. Investigation of models for photosynthetic electron acceptors. Infrared spectroelectrochemistry of ubiquinone and its anions. *FEBS Lett.* 261: 191–195.

Carlà, M., M. Sastre de Vicente, M. R. Moncelli, M. L. Foresti, and R. Guidelli. 1988. Non-conventional normal pulse polarographic techniques with a static mercury electrode for applications at very low reactant concentrations. *J. Electroanal. Chem.* 246:283–296.

Cornell, B. A., M. A. Keniry, A. Post, R. N. Robertson, L. E. Weir, and P. W. Westerman. 1987. Location and activity of ubiquinone 10 and ubiquinone analogues in model biological membranes. *Biochemistry.* 26:7702–7707.

Flewelling, R. F., and W. L. Hubbell. 1986. The membrane dipole potential in a total membrane potential model. Applications to hydrophobic ion interactions with membranes. *Biophys. J.* 49:541–552.

Foresti, M. L., M. R. Moncelli, and R. Guidelli. 1980. Electrode charge measurements at dropping electrodes. Part I. Back-pressure effect and measurement of changes in charge by a potential-step method. *J. Electroanal. Chem.* 109:1–14.

Gordillo, G. J., and D. J. Schiffrin. 1994. Redox properties of ubiquinone (UQ10) adsorbed on a mercury electrode. *J. Chem. Soc. Faraday Trans.* 90:1913–1922.

Guidelli, R. 1971. Chemical reactions in polarography. *In* Electroanalytical Chemistry, Vol. 5. A. J. Bard, editor. Marcel Dekker, New York. 149–374.

Hush, N. S. 1958. Adiabatic rate processes at electrodes. I. Energy-charge relationships. *J. Chem. Phys.* 28:962–972.

Katsikas, H., and P. J. Quinn. 1981. The interaction of coenzime-Q with dipalmitoylcoline bilayers. *FEBS Lett.* 133:230–234.

Katsikas, H., and P. J. Quinn. 1982a. The polyisoprenoid chain length influences the interaction of ubiquinones with phospholipid bilayers. *Biochim. Biophys. Acta.* 689:363–369.

Katsikas, H., and P. J. Quinn. 1982b. The distribution of ubiquinone-10 in phospholipid bilayers. A study using differential scanning calorimetry. *Eur. J. Biochem.* 124:165–169.

Kingsley, P. B., and G. W. Feigenson. 1981. ^{1}H-NMR study of the location and motion of ubiquinones in perdeuterated phosphatidylcholine bilayers. *Biochim. Biophys. Acta.* 635:602–618.

Krishtalik, L. I. 1986. Charge Transfer Reactions in Electrochemical and Chemical Processes. Consultants Bureau, New York.

Ksenzhek, O. S., S. A. Petrova, and M. V. Kolodyazny. 1982. 452-Redox properties of ubiquinones in aqueous solutions. *Biolelectrochem. Bioenerg.* 9:167–174.

Laval, J. M., and M. Majda. 1994. Electrochemical investigations of the structure and electron transfer properties of phospholipid bilayers incorporating ubiquinone. *Thin Solid Films.* 244:836–840.

Läuger, P., R. Benz, G. Stark, E. Bamberg, P. C. Jordan, A. Fahr, and W. Brock. 1981. Relaxation studies of ion transport systems in lipid bilayer membranes. *Q. Rev. Biophys.* 14:513–598.

Lipkowski, J., Cl. Buess-Herman, J. P. Lambert, and L. Gierst. 1986. Mechanism of electron transfer through monomolecular films of neutral organic species adsorbed at an electrode surface. *J. Electroanal. Chem.* 202:169–189.

Miller, I. R. 1981. Structural and energetic aspects of charge transport in lipid layers and biological membranes. *In* Topics in Bioelectrochemistry and Bioenergetics. G. Milazzo, editor. Wiley, Chichester. 194–225.

Mitchell, P. 1976. Possible molecular mechanisms of the protonmotive function of cytochrome systems. *J. Theor. Biol.* 62:327–367.

Moncelli, M. R., and L. Becucci. 1995. The intrinsic pK_a values for phosphatidic acid in monolayers deposited on mercury electrodes. *J. Electroanal. Chem.* 385:183–189.

Moncelli, M. R., L. Becucci, and R. Guidelli. 1994. The intrinsic pKa values for phosphatidylcholine, phosphatidylethanolamine, and phosphatidylserine in monolayers deposited on mercury electrodes. *Biophys. J.* 66:1969–1980.

Moncelli, M. R., L. Becucci, R. Herrero, and R. Guidelli. 1995. Adsorption of tetraphenylphosphonium and tetraphenylborate in self assembled phosphatidylcholine and phoshatidylserine monolayers deposited on mercury electrode. *J. Phys. Chem.* 99:9940–9951.

Moncelli, M. R., and R. Guidelli. 1992. Test of the Gouy-Chapman theory on phosphatidylcholine-coated mercury from differential capacity measurements. *J. Electroanal. Chem.* 326:331–338.

Morrison, L. E., J. E. Schelhorn, T. M. Cotton, C. L. Bering, and P. A. Loach. 1982. *In* Function of Quinones in Energy Conserving Systems. P. L. Trumpower, editor. Academic Press, New York. 35–58.

Nelson, A., and A. Benton. 1986. Phospholipid monolayers at the mercury/water interface. *J. Electroanal. Chem.* 202:253–270.

Ondarroa, M., and P. J. Quinn. 1986. Proton magnetic resonance spectroscopic studies of the interaction of ubiquinone-10 with phospholipid model membranes. *Eur. J. Biochem.* 155:353–361.

Prince, R. C., P. L. Dutton, and J. M. Bruce. 1983. Menaquinones and plastoquinones in aprotic solvents. *FEBS Lett.* 160:273–276.

Quinn, P. J., and M. A. Esfahani. 1980. Ubiquinones have surface-active properties suited to transport electrons and protons across membranes. *Biochem. J.* 185:715–722.

Rajarathnam, K., J. Hochman, M. Schindler, and S. Ferguson-Miller. 1989. Synthesis, location, and lateral mobility of fluorescently labeled ubiquinone 10 in mitochondrial and artificial membranes. *Biochemistry.* 28:3168–3176.

Rich, P. R., and R. Harper. 1990. Partition coefficients of quinones and hydroquinones and their relation to biochemical reactivity. *FEBS Lett.* 269:139–144.

Sánchez, S., A. Arratia, R. Córdova, H. Gómez, and R. Schrebler. 1995. Electron transport in biological processes. II. Electrochemical behavior of Q_{10} immersed in a phospholipidic matrix added on a pyrolitic graphite electrode. *Bioelectrochem. Bioenerg.* 36:67–71.

Schrebler, R. S., A. Arratia, S. Sanchez, M. Hann, and N. Duran. 1990. Electron transport in biological processes. Electrochemical behavior of ubiquinone Q_{10} adsorbed on a pyrolytic graphite electrode. *Bioelectrochem. Bioenerg.* 23:81–91.

Stidham, M. A., T. J. McIntosh, and J. N. Siedow. 1984. On the localization of ubiquinone in phosphatidylcholine bilayers. *Biochim. Biophys. Acta.* 767:423–431.

Takehara, K., H. Takemura, Y. Ide, and S. Okayama. 1991. Electrochemical behavior of ubiquinone and vitamin K incorporated into n-alkanethiol molecular assemblies on a gold electrode. *J. Electroanal. Chem.* 308:345–350.

Ulrich, E. L., M. E. Girvin, W. A. Cramer, and J. L. Markley. 1984. Location and mobility of ubiquinones of different chain lengths in artificial membrane vesicles. *Biochemistry.* 24:2501–2508.

Walz, D. 1979. Thermodynamics of oxido-reduction reactions. *Biochim. Biophys. Acta.* 505:279–353.